

# THE PHYSICAL REVIEW

*A journal of experimental and theoretical physics established by E. L. Nichols in 1893*

---

SECOND SERIES, VOL. 69, NOS. 9 AND 10

MAY 1 AND 15, 1946

---

## Cloud-Chamber Photographs of Heavy Particles at High Altitudes

DONALD J. HUGHES

*Ryerson Physical Laboratory, University of Chicago, Chicago, Illinois*

(Received January 12, 1946)

A series of 5000 cloud-chamber photographs was obtained at an altitude of 15,500 ft., by use of a chamber in a field of 1165 gauss supplied by a permanent magnet. The determination of mass from cloud-chamber photographs of heavily ionizing particles and knock-on electrons is discussed in general and the methods are applied to specific tracks of the present series. It is shown that the errors of mass determination from cloud-chamber data are large but that there is good evidence for a distribution of mesotron masses. The number of slow mesotrons at 15,500 ft. is about equal to the number of slow protons and amounts to 1 percent of the number of fast mesotrons at that altitude. The extremely rapid increase of slow mesotrons with altitude probably means that they are created as such at high altitudes. One photograph, which shows the pair production of low energy mesotrons, is an example of such a process.

### I. INTRODUCTION

THE percentage of slow mesotrons in the cosmic radiation at sea level is so low that hundreds of thousands of cloud-chamber photographs must be taken in order to obtain tracks suitable for mass determination. The number of heavily ionizing, slow mesotrons increases rapidly with altitude, however, and the chances of observing them are correspondingly greater. In order to take advantage of this increase with altitude it was decided to take cloud-chamber photographs at as high an altitude as possible during the 1941 South American cosmic-ray expedition of the University of Chicago.

The work was done at the site of the San Cristobal mine of the Cerro de Pasco Corporation near Cerro de Pasco, Peru. A small building with running water and 110-volt a.c. power was available for cloud-chamber work at an altitude of 15,500 ft. The cloud chamber and associated apparatus was the same as that used earlier for

underground experiments.<sup>1</sup> The chamber, 20 cm in diameter, was mounted in a permanent magnet which supplied a field of 1165 gauss in the chamber, sufficient to deflect heavily ionizing mesotrons. The entire apparatus was about 700 lb. in weight, completely automatic and easily portable. The chamber was counter-controlled by a variety of counter arrangements during the series; however most of the heavily ionizing tracks occurred independently of the counter control. The apparatus was run for a period of three weeks during July 1941 and about 5000 photographs were made.

Although this same chamber when used underground, or at the surface, did not show a single heavily ionizing particle, a fairly large number were observed at the high altitude. Some of the heavy tracks were discussed qualitatively at the cosmic-ray symposium in Rio de Janeiro of

---

<sup>1</sup>V. C. Wilson and D. J. Hughes, *Phys. Rev.* **63**, 161 (1943).

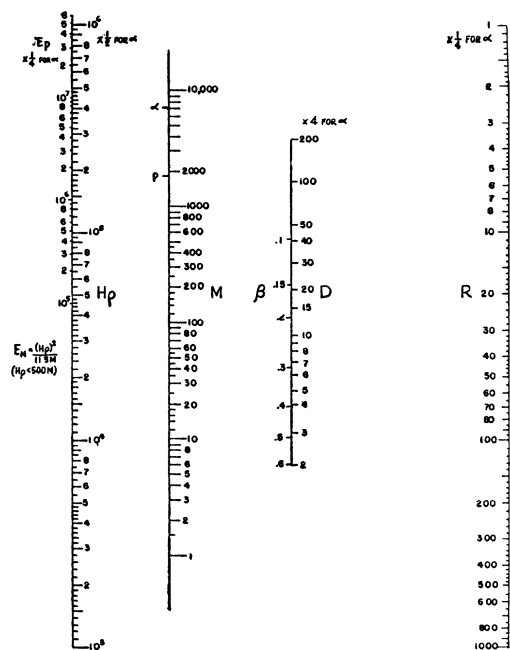


FIG. 1. Nomograph giving magnetic curvature ( $H\rho$ ), velocity ( $\beta$ ), density of ionization ( $D$ ), and range ( $R$ ) for particles of various masses ( $M$ ). Any straight line crossing all the scales gives correct values for the above quantities to a few percent.

August 1941,<sup>2</sup> and a photograph of a pair of slow mesotrons has been published.<sup>3</sup> Unfortunately, war research has delayed the publication of a more complete report until the present time. It is felt, however, that even though the material is rather old by now, the part to be reported here is of sufficient interest to merit publication.

## II. CLOUD-CHAMBER MASS DETERMINATIONS

Particle masses have usually been determined from cloud-chamber photographs by measuring the range or ionization density together with the magnetic curvature of the tracks. A second method which has not been used widely is to measure the energy of an electron ejected by the particle in an elastic collision (formation of a "knock-on" electron). These two methods will be described in general and illustrated by specific cases from the present work.

### A. Mass Determination by Increased Ionization

If a particle has low enough energy so that its velocity is significantly less than that of light

<sup>2</sup> D. J. Hughes, Acad. Bras. de Ciencias **67** (1941).

<sup>3</sup> D. J. Hughes, Phys. Rev. **60**, 414 (1941).

( $\beta < 1$ ), then its ionization density increases and its mass may be determined from any two of the three quantities, curvature in a magnetic field, density of ionization, and range. Perhaps the simplest way to picture the dependence of mass on the three quantities is by a nomograph of the type published by Corson and Brode.<sup>4</sup> Such a nomograph is shown in Fig. 1. It is modeled after Corson and Brode's but has been extended to cover all masses from electrons to alphas and also to cover a greater range of  $H\rho$  and range values. Any straight line crossing all the scales connects consistent values of  $H\rho$  (magnetic field  $\times$  radius of curvature), density of ionization  $D$  (where minimum value for a fast particle = 1), velocity  $\beta$ , and range  $R$  (cm of air), for a given mass  $M$  (mass of electron = 1). A scale  $E$  gives the kinetic energies of protons in electron volts, and if multiplied by  $\frac{1}{4}$ , the energies for alphas. Energies for other  $M$ 's can be obtained from the formula shown at the left. The  $H\rho$ ,  $D$ , and  $R$  scale readings must be multiplied by the factors shown for alphas.

Of course a chart covering such a wide range of variables cannot be precise at all points. It has been designed, however, in such a way that the errors are not excessive for any particular combination of variables. Thus, for protons the range as a function of energy is 9 percent low at 2 cm (by comparison with the curves of Livingston and Bethe<sup>5</sup>), becomes exact at intermediate ranges, and is 9 percent high at 260 cm (the greatest range shown in Livingston and Bethe's curves). For alphas (again by comparison with Livingston and Bethe) the variation is from 12 percent low at about 2 cm to about 4 percent high at 20 cm. For a mesotron of mass 200 the ranges (as a function of  $H\rho$ ) when compared to those given by Rossi and Greisen<sup>6</sup> are high by 10 percent for the shortest ranges, by 5 percent at about 30 cm, and agree at 800 cm. Electron ranges as a function of  $H\rho$  from the chart lie within the spread of the experimental determinations of electron ranges from 1 to 100 cm (even though the rule that the straight line on the chart must cross *all* the scales

<sup>4</sup> D. R. Corson and R. B. Brode, Phys. Rev. **53**, 776 (1938).

<sup>5</sup> M. S. Livingston and H. A. Bethe, Rev. Mod. Phys. **9**, 245 (1937).

<sup>6</sup> G. Rossi and K. Greisen, Rev. Mod. Phys. **13**, 240 (1941).

is violated in this case). Although the above errors of the chart are not small, they are smaller in general than the inherent uncertainty of the mass determinations which are discussed below. Figure 1 then turns out to be sufficiently accurate for calculations involving mass determinations from typical cloud-chamber photographs for masses from electrons to alphas, and its use is justified by simplicity.

Range can perhaps be measured most accurately of the above quantities if the particle stops in the gas of the chamber. The density of ionization depends on several variable conditions of the chamber and can only be estimated unless delayed droplet counting is done, and the  $H\rho$  value is affected by chamber distortion at high energies and by scattering at low energies. For any measured  $H\rho$  value there is always a variation in true radius of curvature due to the spurious radius,  $\rho_s$ , caused by scattering which must be added to the uncertainty of measurement of the  $H\rho$  value. Williams<sup>7</sup> has given a formula for the average  $\rho_s$  which can be reduced to a simple form applicable to the present chamber, and accurate to a few percent for the region covered by Fig. 1. For  $H=1165$  gauss, argon gas at a pressure of 80 cm, and a track length of 16 cm we have

$$\rho_s/\rho = 15.0\beta, \tag{1}$$

which shows that for fast particles  $\rho_s$  causes a 7 percent error in  $\rho$ , and that for  $\beta=0.067$  the spurious curvature is equal to the magnetic curvature itself. Thus even though particles of low momentum can have their curvature measured more easily, the error due to scattering will be greater and the accuracy of mass determination actually less for the slower particles.

For a given chamber gas, magnetic field, and particle mass there is a certain curvature value for which the accuracy of mass determination is a maximum. Figure 2 shows the variation in accuracy of mass determination as a function of  $\rho$  for the present chamber as a typical example. It is assumed that the error in measuring radius of curvature (due to convection currents, etc.) is equal to a displacement of the center of the track of 0.05 cm, this value being based on tracks measured with no magnetic field in the present

chamber. The curves marked "fixed  $D$ " show the probable error of the mass values (for an actual mass of 200) which would result when the mass is determined from  $D$  (assuming no error in  $D$ ) and  $H\rho$ . The curves marked "fixed  $R$ " are the probable error when mass is determined from measured  $R$  (assuming no error) and  $H\rho$ . The results were calculated from Fig. 1 and Eq. (1).

It is seen that the accuracy of mass determination is greatest for a radius of curvature of about 125 cm (range of 500 cm) and that it is greater for a determination based on a measured  $D$  than on a measured  $R$  (assuming no error in measurement of  $D$  and  $R$ ). Even at best, however, the mass would be  $200(+50, -32)$ . With twice the magnetic field the most accurate point will occur at the same  $H\rho$  value (and same range) but the corresponding radius of curvature will be half and the accuracy of mass determination will be doubled. Space does not permit a discussion of the effect of other changes on the accuracy such as the effect of change of chamber gas, change of pressure, use of absorbers in determining  $R$ , etc., but they can easily be calculated in a manner similar to that used in calculating Fig. 2. In this connection it is useful to remember that  $\rho_s/\rho$  changes very nearly as  $l^{\frac{1}{3}}$  (where  $l$  is track length), as  $z^{-1}$  ( $z$ , atomic number of chamber gas), as  $p^{-\frac{1}{2}}$  ( $p$ , chamber pressure), and as  $H$ .

It is obvious that the inherent errors in mass determination with the cloud chamber are large enough so that the errors in the chart of Fig. 1 are much less and its use is justified in such measurements. In the photographs taken in the present

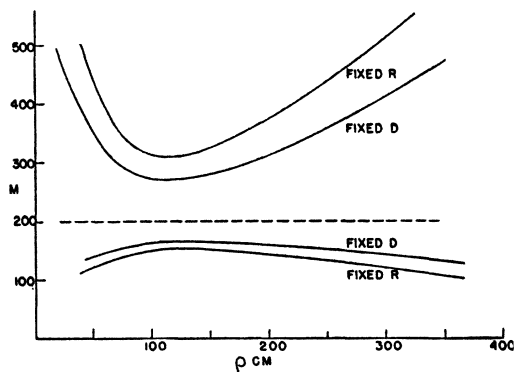


FIG. 2. Variation in measured mesotron mass ( $M$ ) as a function of radius of curvature for a true mass of 200. Curves labeled "fixed  $D$ " refer to measurements based on density of ionization; "fixed  $R$ " to those based on range.

<sup>7</sup> E. J. Williams, Phys. Rev. 58, 292 (1940).

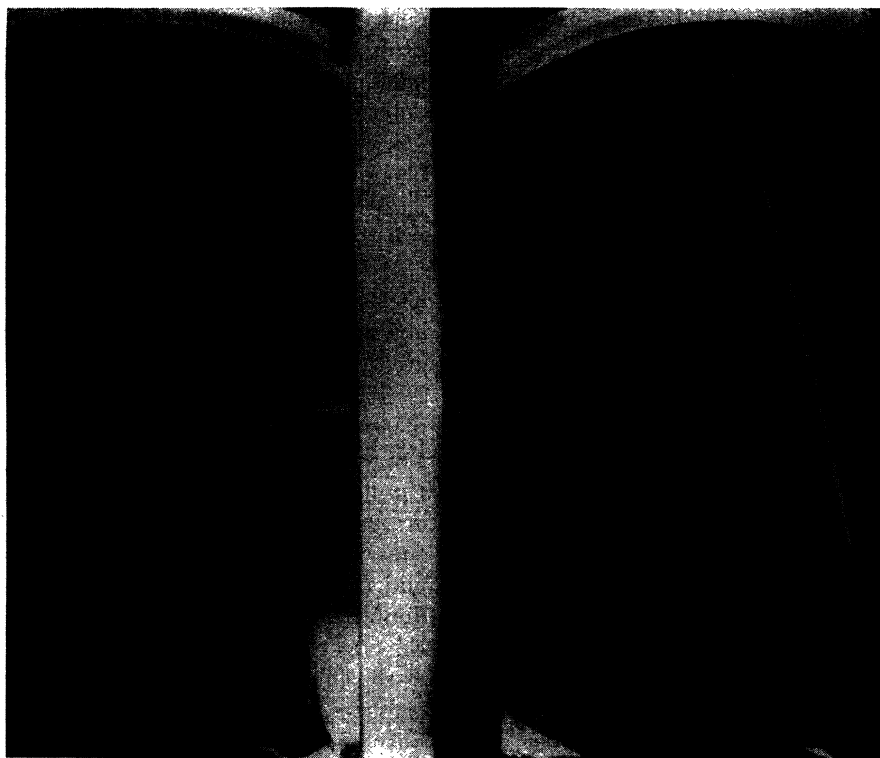


FIG. 3. Stereoscopic views of a positively charged particle whose curvature, density, and range identify it as a proton, of energy about 3 Mev.

series about 50 tracks were observed which ionized heavier than electronic tracks yet showed some curvature in the magnetic field. Some 20 of them were of a quality to justify mass determinations, and several of these tracks will be described here.

Figure 3 is a stereoscopic view of a heavily ionizing particle of positive sign. It is almost exactly in the center of the illuminated portion of the chamber throughout its length and appears to end in the chamber. However, the end of the track is not visible in the right view (obscured by a light baffle) so it is not completely certain that the track does not scatter sharply out of the illumination and pass out of the chamber. The  $H\rho$  value measured at the central region (residual range 12 cm) is  $1.7 \times 10^5$  gauss cm (there is some distortion at the upper rim of the chamber and several scatterings along the track). The ionization is so heavy that discrete blobs of ionization cannot be seen; however, by comparison with slow electrons and fast alphas it is possible to

estimate that the density is at least 30 and probably 50–100. Figure 1 shows that the above values of  $H\rho$ ,  $D$ , and  $R$  are consistent and indicate a mass roughly 1300. Therefore, the particle is probably a proton, and the probable variation in  $H\rho$  from Eq. (1) is from  $9 \times 10^4$  to  $10^6$ . If the values  $R=12$ ,  $D=50-100$ , and  $H\rho=9 \times 10^4-10^6$  are marked on Fig. 1, it is seen that the particle can certainly be identified as a proton but that its actual mass cannot be precisely determined. Inclusion of the uncertainty in  $H\rho$  due to  $\rho_s$  increases the uncertainty of the mass determination by a large amount.

The lower track in Fig. 4 is positive (assuming it is moving downward) with an  $H\rho$  of  $1.05 \times 10^5$ . It does not ionize as heavily as the proton of Fig. 3 (the discrete blobs are just visible); its density, by comparison with slow electrons, is approximately 10. It does not stop in the chamber so it can be said only that its range is certainly greater than 14 cm air. Figure 1 shows the consistency of the above values with a mass about

250. A mass of 250 then gives a range in  $H\rho$  due to  $\rho_s$  of 0.82 to  $1.46 \times 10^5$ . This range in  $H\rho$  is about the minimum to be expected for the track has a radius of curvature of 90 cm (see Fig. 2) but the corresponding uncertainty in  $M$  is from 200 to 350 even if we assume no error in  $D = 10$ . If the  $D$  value is between limits of 6 and 15, then the  $M$  value will vary even more, from 140 to 440. This track is certainly a mesotron, and of mass about 250, but with a large experimental uncertainty.

As mentioned in the introduction, one photograph of this series has already been published<sup>3</sup> which is quite certainly that of a mesotron pair produced in the material of the cloud chamber. The measurements have now been rechecked with the result that the mass of the right-hand member of the pair has been lowered from 180 to 160 (as judged by  $H\rho$  and  $D$ ) with a range due to uncertainty in curvature and ionization of 120 to 230 for the mass value. The knock-on electron (see below) observed on this track gives a mass value of 190 (+85, -50). Combination of the two estimates indicates a mass of 175 (+55, -30) for

the particle. The mass of the second member of the pair can best be estimated simply by comparison with the first, for its  $H\rho$  and  $D$  are very nearly the same, thus it seems likely that its mass is also about 175.

Figure 5 shows a track that is heavily ionizing but of unusually great curvature. The heavy verticle white band resulted from a wire in the developing tank which prevented a strip from being completely cleared by the hypo—the complete track in the right-hand view is easily visible on the negative however. The track enters the illumination at the right and stops at the left end which is in the full illumination; it is therefore negative. The  $H\rho$  at the center (where the residual range is 1.8 cm of air equivalent) is  $4.1 \times 10^3$ . The track is slightly blurred by age but its ionization density is estimated to be in the range 15 to 40. From Fig. 1 the range and curvature give a surprisingly small mass of 14, which, however, is consistent with the ionization density. If the effect of  $\rho_s$  is now calculated, it is found to be so large (because of small  $H\rho$  and short track length)



FIG. 4. A positive mesotron of mass approximately 250.



FIG. 5. A negative mesotron whose curvature, density, range, and scattering show that it has an unusually low mass of 30.

that it is necessary to take into account the variation of  $\rho_s$  with  $H\rho$  and  $\beta$ . When this is done, it is found that all mass values between 6 and 50 could give the observed  $H\rho$  and  $R$ . However, the ionization density indicates  $M$  is at least 10 and probably about 25. The scattering is much less than that of an electron which has a very erratic path when its residual range is 2 cm. As  $\rho_s$  for a

particle of given range increases with  $M^{\frac{1}{2}}$ , the latter quantity must be large compared to unity in this case, say at least 5, which would mean an  $M$  of at least 25. If all the above values are marked on Fig. 1, it seems that the mass is probably about 30 but definitely in the range 10 to 50.

The heavily ionizing track in the lower left-

TABLE I. Mass determinations from  $H\rho$ ,  $R$ , and  $D$ .

Number	Sign	$H\rho$	$D$	$R(\text{cm air})$	$M$	Remarks
1 (Fig. 5)	-	$4.1 \times 10^3$	15-40	1.8	$30(+20, -20)$	
2	+	$3.7 \times 10^4$	15-30	13	$140(+220, -60)$	
3	-	$1.03 \times 10^5$	4-6	10	$175(+55, -30)^*$	Mesotron pair <sup>a</sup>
4	+	$1 \times 10^5$	4-6	10	$175(+140, -60)$	
5 (Fig. 4)	+	$1.05 \times 10^5$	6-15	20	$250(+190, -110)$	
6	-	$6.4 \times 10^4$	20-40	14	$250(+380, -100)$	
7	+	$2.8 \times 10^5$	2-4	30	$270(+330, -110)$	
8	?	$>3 \times 10^5$	15-30	14	$>900$	
9	+	$2.3 \times 10^5$	$>20$	30	$>1100$	
10 (Fig. 3)	+	$1.7 \times 10^5$	50-100	12	$1300(+2000, -400)$	
11	?	$>2 \times 10^5$	$>40$	8	$>1200$	
12 (Fig. 6)	?	$>10^6$	20-50	14	$\sim 10 \times \text{proton}$	$Z \sim 5$
13	?	$>10^6$	20-50	10	$\sim 10 \times \text{proton}$	

\* Knock-out determination (No. 2 of Table II) included in  $M$  value.

<sup>a</sup> See reference 3.

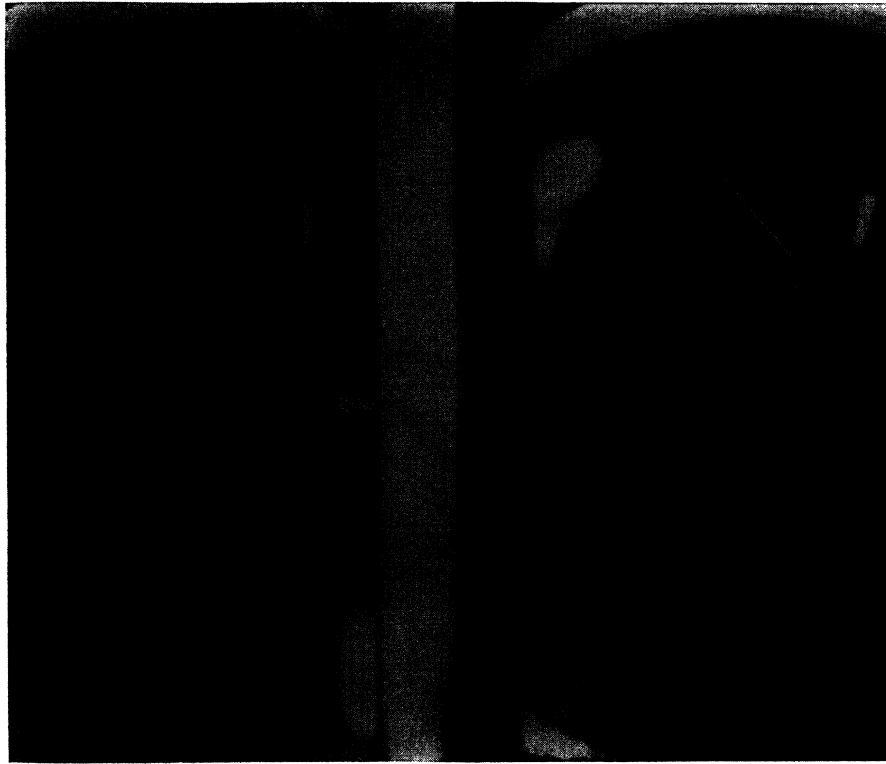


FIG. 6. The track in the lower left corner creates an extremely large number of knock-on electrons. It is identified as a high energy particle of charge about 5.

hand corner of Fig. 6 is unusual in that five knock-on electrons are visible along the illuminated track length of 11 cm air equivalent. The track is sloping so that the upper end is back of the illuminated space and is not visible. The  $H\rho$  value is too great to be measured. It has already been found with the present chamber<sup>1</sup> that the number of knock-on electrons per cm track length for fast particles ( $\beta=1$ ) was  $6.8 \times 10^{-3}$ , a value which checked the theoretical estimate. The present track, however, has 0.45 per cm, or 67 times the above value. It is true that the probability of ejection of knock-on electrons increases with decreasing  $\beta$  (as  $1/\beta^2$ ), however, the maximum transferable energy decreases [as  $\beta^2/(1-\beta^2)$ ] and becomes so low for heavily ionizing tracks that knock-ons are not seen as discrete tracks along slow ( $\beta < 0.1$ ) mesotron, proton, or alpha tracks. The present track then cannot be a mesotron, proton, or alpha because its large  $D$  is inconsistent with the high knock-on energy.

It is possible to reconcile the frequency of knock-ons and large ionization density of the track (which require a low  $\beta$ ) with the relatively high knock-on energy (which requires a high  $\beta$ ) by assuming that the charge on the particle is high. If  $\beta$  is taken as 0.7 and the particle's charge as 5, then  $D$ , which would be 1.5 for  $Z=1$  be-

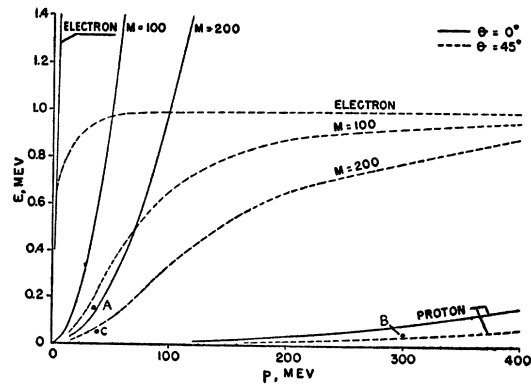


FIG. 7. The energy of knock-on electrons ( $E$ ) as a function of primary momentum for different primary masses and angles of ejection of knock-ons.

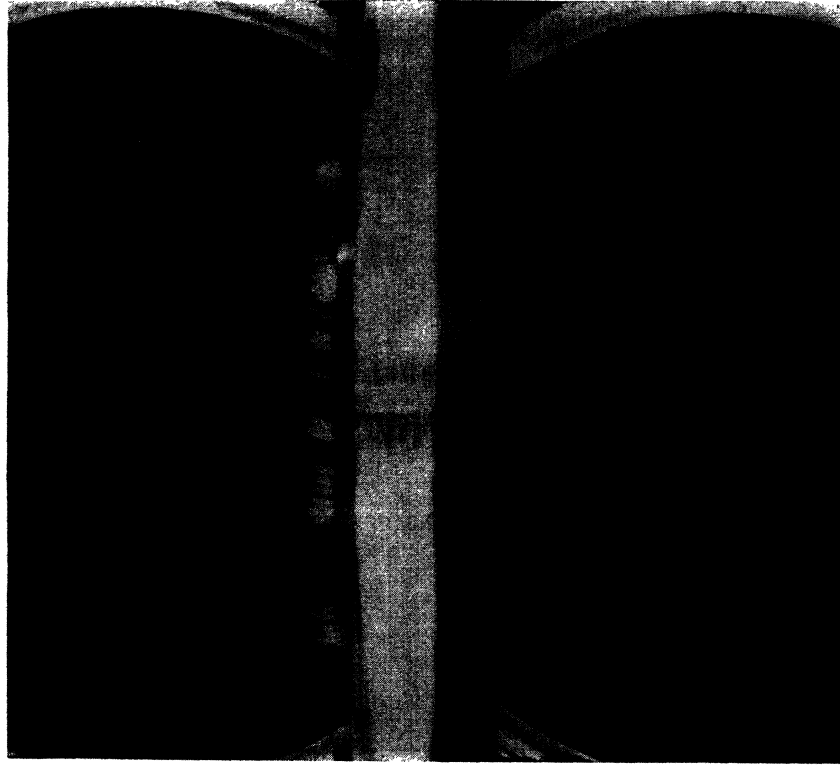


FIG. 8. A mesotron whose mass is estimated as 180 from primary momentum, energy of knock-on electron and angle of ejection of knock-on. The mesotron is not visible beyond the point (center of the chamber) where the knock-on is created.

comes  $1.5 \times 5^2 = 37$ , while the high  $\beta$  value means that the maximum energy transferable to a knock-on is 960 kev and the average observable knock-on energy about 25 kev. The above values for  $D$  and knock-on energy agree well with the observed track (average knock-on energy = 15–20 kev,  $D = 30$ –50). The probability of ejection of knock-ons will be  $Z^2/\beta^2 = 50$  times that of fast particles in comparison with the observed 67. The above arguments are independent of the mass of the unknown particle which would presumably be large because of the high  $Z$ . Its energy would be about  $2 \times 10^8 A$  where  $A$  is its atomic weight; thus, if it were a boron 10 nucleus, for instance, it would have an energy of 2000 Mev at which energy it would most certainly have a charge of 5. One other track very similar to that of Fig. 6 was observed during the run and is probably to be interpreted in a similar manner.

Other mass determinations based on  $H\rho$ ,  $D$ , and  $R$  will not be described in detail but are summarized along with those above in Table I,

which will be discussed following the description of the knock-on measurements below.

### B. Mass Determination by Knock-On Energy

Although the frequency of occurrence of knock-ons and their energy distribution are independent of the mass of the primary particle (provided the energies are less than the maximum transferable energy), the mass can be obtained for a particular collision if the angle of ejection and energy of the electron as well as primary momentum can be measured. In contrast to the ionization method, the knock-on method can be used where the primary momentum is so high that no increased ionization is exhibited. However, in order to attain accuracy in mass determination the collision must be almost head-on and the primary momentum somewhat low. The formula involved is

$$E = 2mc^2 \frac{p^2 \cos^2 \theta}{\{[p^2 + (Mmc^2)^2]^{1/2} + mc^2\}^2 - p^2 \cos^2 \theta}, \quad (2)$$

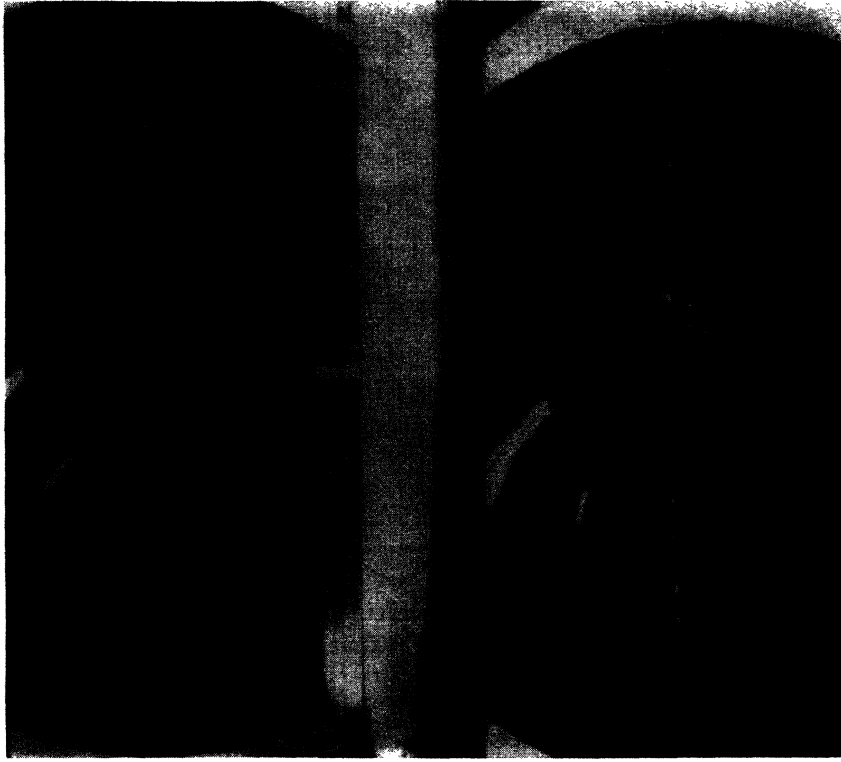


FIG. 9. A low energy knock-on caused by a proton primary.

where  $E$  is the knock-on energy,  $mc^2$  the electron rest energy,  $\theta$  the angle of emission, and  $p/c$  the momentum ( $p = 300H\rho$ ) of the primary of mass  $Mm$ . Figure 7 shows the variation of  $E$  with  $p$  for different  $M$ 's and  $\theta$ 's. For  $\theta = 0$  (head-on collision) mass discrimination is quite good for all values of  $p$ ; however, such collisions are very rare. For  $\theta = 45^\circ$  the best  $p$  values are about  $10^8$  ( $H\rho = 3 \times 10^5$ ); at higher momenta electrons cannot be distinguished from mesotrons. For angles greater than  $60^\circ$  the knock-on energies become small as does the accuracy of mass determination.

In Fig. 8 is shown a knock-on from which a mass estimate may be made. The primary passes out of the illumination at about the point where the knock-on is ejected; its  $H\rho$  is  $1.3 \times 10^5$ . The angle  $\theta$  is  $18^\circ$ ; hence the collision is nearly head-on ( $\cos^2 \theta = 0.9$ ). The energy of the knock-on can be obtained by measuring its range in the chamber (30 cm air equivalent) or its  $H\rho$  value ( $1.4 \times 10^3$ ). The range and  $H\rho$  values are consistent (Fig. 1) and the energy of the electron is 150 kev. Point  $A$  on Fig. 7 corresponds to this knock-on

electron, and it is clear that the primary must be a mesotron; Eq. (2) actually gives  $M = 180$ . The principal uncertainty is in the measurement of  $H\rho$ , which was unfortunately difficult in this case. It leads to an uncertainty in mass of about  $(+90, -50)$ . A better curvature measurement for this knock-on could give a much better mass determination for the exact  $\theta$  is not critical and the energy of the electron can be measured accurately.

The knock-on of Fig. 9 is of low energy (50 kev by range) but the primary is of high momentum; because of distortion at the ends only a lower limit of  $1.0 \times 10^6$  for  $H\rho$  can be given. The angle  $\theta$  is about  $50^\circ$ . The above values are shown in Fig. 7 as  $B$  which falls close to the  $45^\circ$  curve for protonic mass, and Eq. (2) gives a lower limit of 1300 for  $M$ . The uncertainty in  $H\rho$  measurement for this high momentum particle makes exact mass measurement impossible, but the identification as a proton is quite certain. Figure 1 shows that the particle has a velocity low enough so

TABLE II. Mass determinations from knock-on electrons.

Number	Sign	$H\rho$	Electron energy (kev)	$\theta$	$M$	Remarks
1	—	$1.3 \times 10^5$	150	$18^\circ$	180(+90, -50)	
2	—	$1.03 \times 10^5$	34	$50^\circ$	190(+85, -50)	Same track as No. 3 of Table I
3	—	$3 \times 10^5$	130	$53^\circ$	280(+250, -80)	
4	—	$3.6 \times 10^5$	300	$30^\circ$	340(+300, -100)	
5	?	$> 1 \times 10^6$	50	$50^\circ$	$> 1300$	
6	+	$\sim 9 \times 10^5$	48	$45^\circ$	$\sim 1800$	
7	?	$> 1 \times 10^6$	33	$40^\circ$	$> 1500$	

that the ionization is somewhat greater than unity, about 2-4.

A knock-on due to a mesotron primary obtained in the present series has already been described<sup>3</sup> in connection with a mesotron pair. The electron energy is 34 kev, its angle  $50^\circ$  and the primary  $H\rho$  is  $1.03 \times 10^5$ . These values are plotted as  $C$  in Fig. 7 and a mesotronic mass of about 200 is indicated. Actual calculation from Eq. (2) if we allow for uncertainty in  $H\rho$  due to scattering gives  $M = 190(+85, -50)$ . As discussed in Section II A, the knock-on mass determination for this particle agrees well with that based on the ionization density. Both methods have their main source of inaccuracy in the uncertainty of  $H\rho$  which is due, at  $H\rho = 10^5$ , about equally to  $\rho_s$  and to experimental error in the actual curvature measurement due to distortion.

The mass determinations from knock-ons discussed above, together with several others from the present series, are summarized in Table II. In general it can be said that the knock-on determinations have no great inherent inaccuracy, but require a higher magnetic field for more precise  $H\rho$  measurements in order to utilize the higher momentum tracks which are otherwise suitable for the knock-on method.

### III. DISCUSSION OF RESULTS

The 19 tracks of Tables I and II can be divided without much doubt into 10 mesotrons (4+, 6-), 7 protons, and 2 heavier particles. The approximate equality of the number of slow mesotrons and protons means that the area of the mesotron momentum spectrum below  $10^8$  ev is about equal to that of the proton momentum spectrum below  $10^9$  ev. The values of the mesotron masses vary from 30 to 340 (plus experimental error). Even

though it is true that each mass determination is subject to a large uncertainty it seems difficult to reconcile all the measured mass values with a unique mesotron mass. It is true that most of the values are in the 200 region but track 1 of Table I is very good evidence for the existence of "light mesotrons" of mass much less than the customary 200. Wheeler and Ladenburg<sup>8</sup> in a 1941 review concluded that the experimental evidence at that time was insufficient to "allow a decision of the very important question whether the mass of the meson is unique" but the present results seem to indicate a distribution of mesotron masses.

Most of the tracks of Table I are not those which tripped the counter control of the chamber but simply occurred in the chamber by chance when it expanded. Hence the rate of occurrence, 13 measurable cases in 5000 pictures, refers mainly to the chance rate of occurrence of such tracks in the cloud chamber. If we wish to compare the relative numbers of slow and fast mesotrons, for instance, we must compare the observed heavy tracks with the chance rate for fast mesotrons rather than with the number of fast particles in the chamber, for the latter are counter-controlled. The total "sensitive time" of the cloud chamber for the whole series of pictures can be estimated to be about 450 sec., that is, in addition to the counter control tracks which were observed, all those particles which pass through the chamber in 450 sec. were also observed. The number of fast mesotrons which traverse the chamber can be calculated from the number observed in the experiments of Schein, Jesse, and Wollan<sup>9</sup> at an equal altitude, taking into account

<sup>8</sup> J. A. Wheeler and R. Ladenburg, Phys. Rev. 60, 754 (1941).

<sup>9</sup> M. Schein, W. P. Jesse, and E. O. Wollan, Phys. Rev. 59, 615 (1941).

the geometrical difference between their counter set and the cloud chamber. The result, for mesotrons of range greater than 8-cm lead (i.e., for those above the energy of minimum ionization loss) is that 900 fast mesotrons pass through the chamber in 450 sec. Approximately the same result is obtained from the known rate of occurrence of chance mesotrons in the chamber at sea level (from earlier experiments) and the increase of mesotrons with altitude.<sup>9</sup>

As there were 9 slow mesotrons observed which were not counter-controlled, the ratio of slow (heavily ionizing) mesotrons to fast is 0.01. It is obvious that this ratio is far greater than that at sea-level where, for example, Johnson and Shutt<sup>10</sup> obtained one heavily ionizing particle among 42,000 fast tracks of 50-cm length. Herzog<sup>11</sup> also finds a striking increase of heavily ionizing particles with altitude. He reports that tracks identifiable as slow mesotrons begin to occur at 15,000 ft. and above 25,000 ft. constitute 10 percent of the fast tracks. If it is assumed that the slow mesotrons result only from the slowing

down of the fast, then the change of the fast spectrum with altitude could not account for the observed great increase of slow mesotrons with altitude. It seems likely, therefore, that the slow mesotrons observed at high altitudes are created as such and that the process, practically non-existent at sea level, becomes more and more evident with increasing altitude. The slow mesotron pair<sup>3</sup> photographed during the present experiment is an example of such a process. It is noteworthy, however, that Schein, Jesse, and Wollan<sup>9</sup> found no evidence for slow mesotrons in their flights with thin (4-6 cm) lead absorbers.

It is a pleasure for the writer to acknowledge the inspiring leadership of Dean A. H. Compton during the progress of the above work. The Cerro de Pasco Corporation is to be thanked for the use of many facilities during our stay at San Cristobal and the Academy of Science of Brazil for the cordiality extended to us at the cosmic-ray symposium in Rio De Janeiro, August 3-9, 1941. Mr. Paul Ledig of the Huancayo Observatory and Professor Julio Hubner of San Marcos University were of great assistance during the mountain observations, as were Dr. L. Seren and Mr. E. Strugala of the University of Chicago in the interpretation of the data.

---

<sup>10</sup> T. H. Johnson and R. P. Shutt, *Phys. Rev.* **61**, 381 (1942).

<sup>11</sup> G. Herzog, *Phys. Rev.* **59**, 117 (1941).

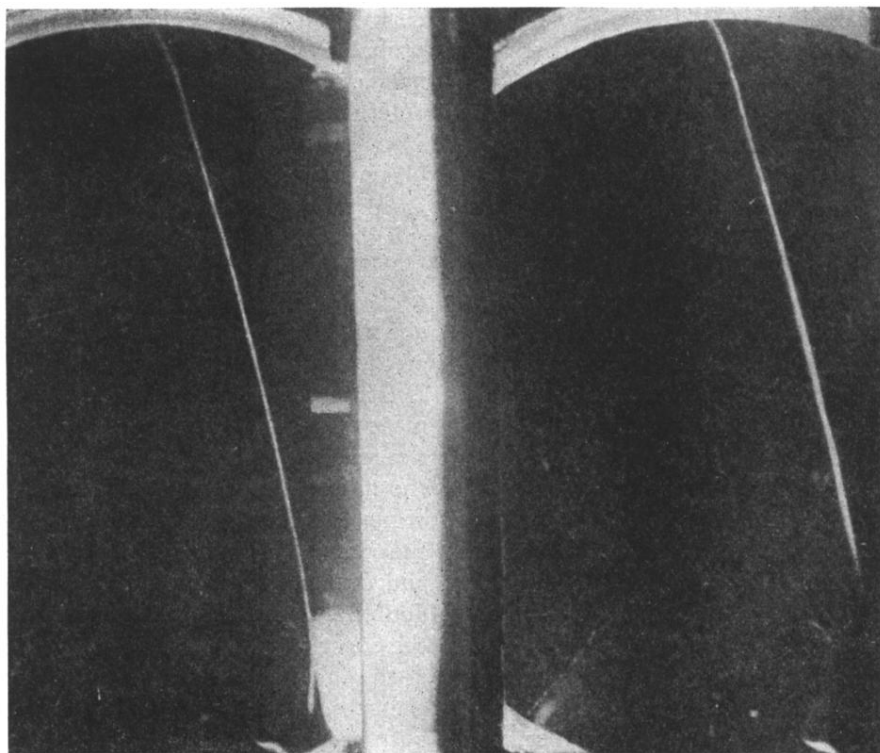


FIG. 3. Stereoscopic views of a positively charged particle whose curvature, density, and range identify it as a proton, of energy about 3 Mev.

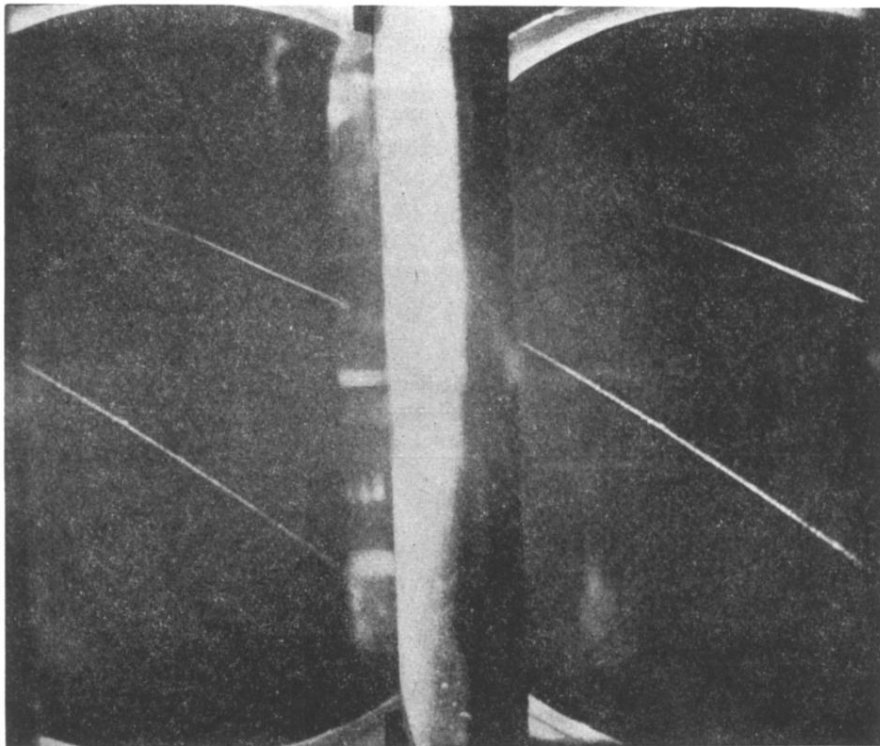


FIG. 4. A positive mesotron of mass approximately 250.

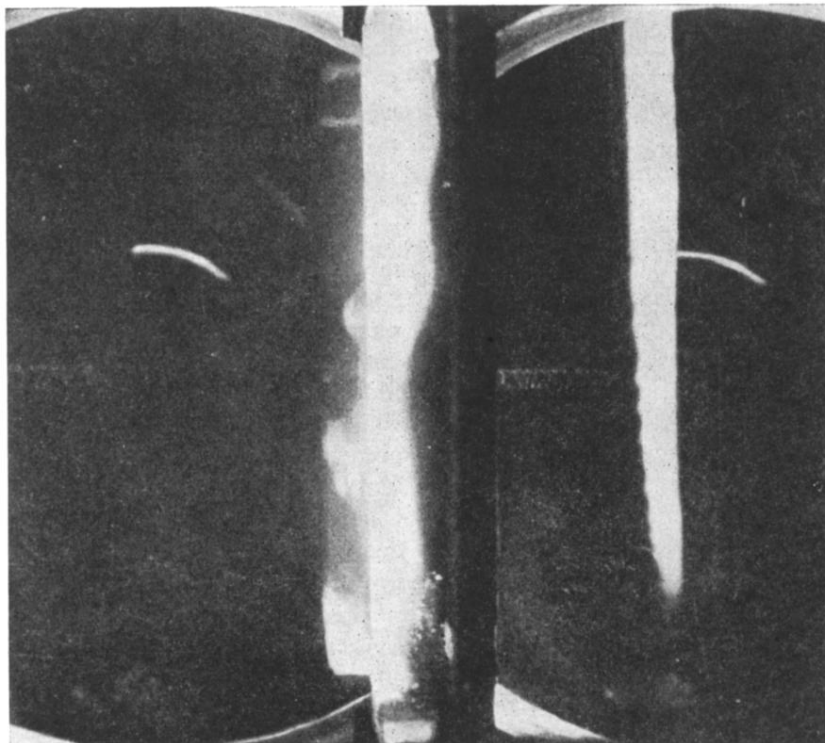


FIG. 5. A negative mesotron whose curvature, density, range, and scattering show that it has an unusually low mass of 30.

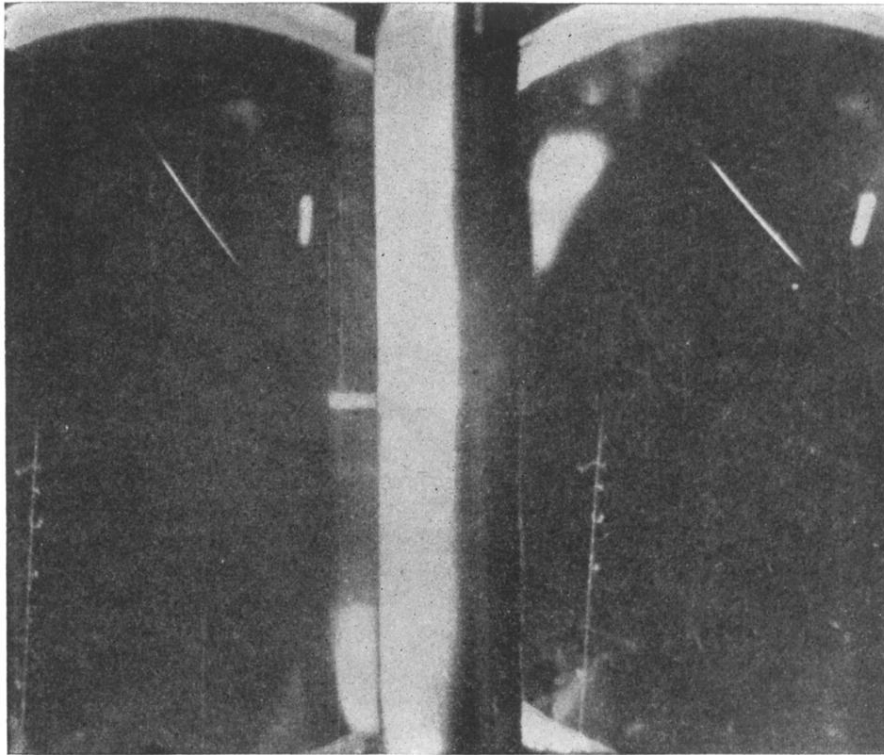


FIG. 6. The track in the lower left corner creates an extremely large number of knock-on electrons. It is identified as a high energy particle of charge about 5.

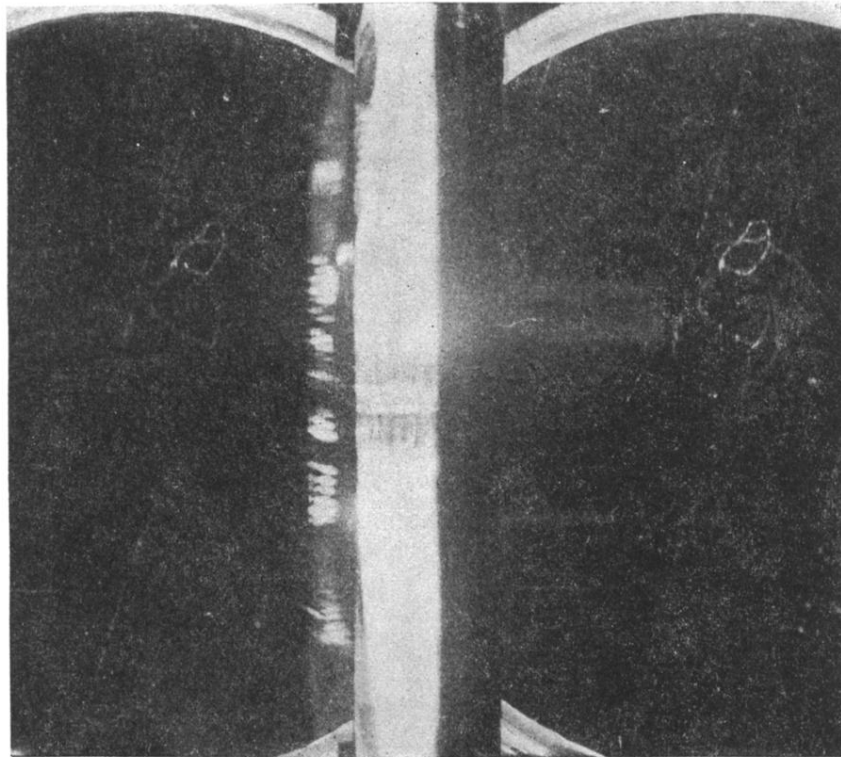


FIG. 8. A mesotron whose mass is estimated as 180 from primary momentum, energy of knock-on electron and angle of ejection of knock-on. The mesotron is not visible beyond the point (center of the chamber) where the knock-on is created.

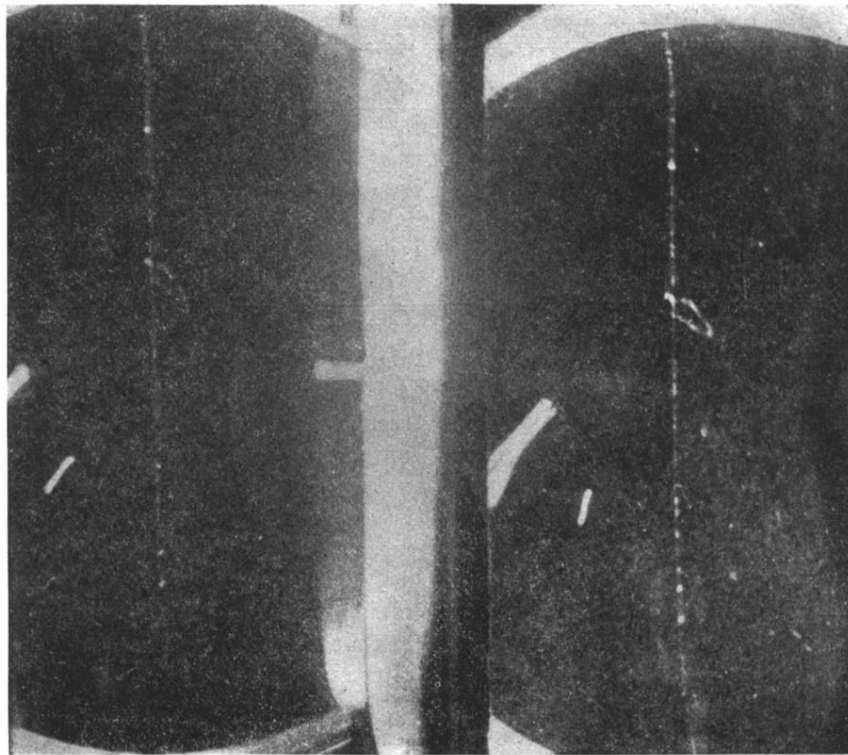


FIG. 9. A low energy knock-on caused by a proton primary.